Interdisciplinary Research Review
Volume 15, Number 5, Pages 1 – 7

Soil water retention curve and permeability function of the para rubber biopolymer treated sand

Arun Lukjan*, Arsit Iyaruk, and Chumnong Petchprakob

Department of Civil Engineering, Faculty of Engineering, Rajamangala University of Technology Srivijaya, Songkhla, Thailand

Abstract

Unsaturated flow phenomena impact all the geotechnical engineering applications. Requirements the understanding include seepage, shear strength, and volume change behaviors of unsaturated soil are important. Since several researchers have put efforts to conduct a potential of biopolymer for soil improvement for the last decade. This paper aimed to conduct a comprehensive experimental study on soil water retention curve (SWRC) and a permeability function prediction of para rubber (PR) biopolymer treated sand. Sand-para rubber (SPR) mixtures were prepared with sand being the base material and with different PR contents (15%, 17.5%, 20%, and 22.5%). A series of laboratory tests were conducted including the filter paper method and falling head test. The results showed that the wetting SWRC of the four SPR mixtures is significantly different compared with untreated sand which tends to give a higher value of saturated volumetric water content and water entry suction. The permeability test result displayed that the values of saturated hydraulic conductivity decreased with increasing PR content. The shape of the unsaturated hydraulic conductivity curve is quite similar for all SPR mixtures but values vary in three orders of magnitudes compared with a value of untreated sand. This experimental study showed the remarkable effectiveness of the in the wetting SWRC shape and hydraulic conductivity function of the poorly graded sand. The results also indicated that the para rubber significantly influenced on the pore size distribution of the SPR mixtures.

Keywords: para rubber, soil suction, water content, hydraulic conductivity, biopolymer
Article history: Received 5 May 2020, Revised 10 August 2020, Accepted 10 August 2020

1. Introduction

The majority of geotechnical engineering applications occur in the vadose zone. Unsaturated soil applications include foundations, excavation, landslide, compacted soil, and contaminant migration [1]. Since the main aims of ground improvement can be summarized as follows: to increase bearing capacity, decrease settlement, control shrinking and swelling, control permeability, and reduce susceptibility to liquefaction [2]. While, the unsaturated soil problems require the understanding of broad behavior include seepage, shear strength, and volume change behaviors. The last decade has seen significant growth of research on biopolymer (e.g., starch, beta-glucan, xanthan gum, gellan gum, agar, polyacrylamide, and guar gum) application to geotechnical engineering, especially for soil stability and improvement purposes [3]. Researchers have found that biopolymers are an alternative to conventional construction materials and soil stabilization. For instance, that can enhance the shear strength characteristic [4-6], mitigating seismic-induced liquefaction [7], erosion resistance [8-9], and decreased hydraulic conductivity [10-11] of granular soil.

Natural rubber latex (herein referred to para rubber, PR), an elastomer that was originally derived from the sap of para rubber plant, has been successfully used as a civil engineering material. An advantage property of para rubber comprises excellent dynamic properties with a low hysteresis loss, good low-temperature properties, strong bonding, and high resistance to tear and abrasion. For geotechnical engineering works, many efforts on investigating a potential of PR used as an admixture in soil improvement have been carried out on shear strength behavior [12], mechanical properties of geosynthetic clay liner [13], para rubber soil-cement road [14], and drought relieving water pond [15]. These study results suggest the potential utility of PR as a cementation material for geotechnical engineering purposes. Nevertheless, the previous studies did not explore associate with unsaturated soil context.

The constitutive relationship between water content or degree of saturation and matric suction of unsaturated soil represents by the soil water retention curve

*Corresponding author; email: federun9@gmail.com

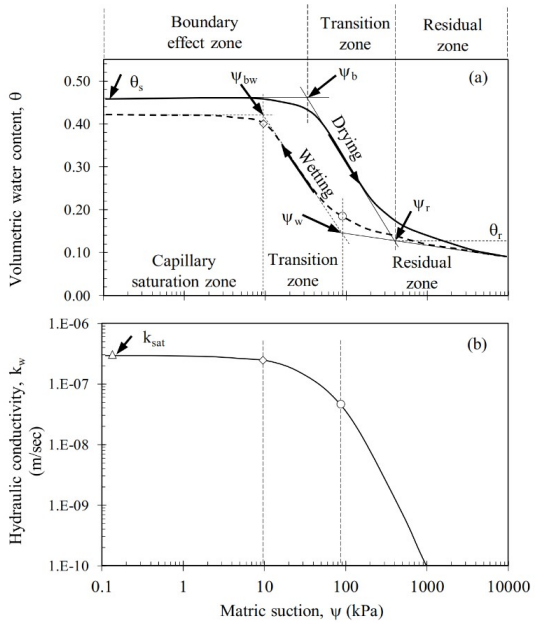

Figure 1: Typical (a) SWRC and (b) unsaturated hydraulic conductivity function.

(SWRC). SWRC is also referred to as soil water characteristic curve or capillary pressure curves. While in unsaturated soil, hydraulic conductivity is the most crucial parameter which affected on flow process in this zone. Fig. 1a illustrates a typical SWRC that includes drying (desorption) and wetting (adsorption) processes associated with unsaturated hydraulic conductivity varies with soil suction as shown in Fig. 1b. There are various devices and techniques for measuring soil suction of unsaturated soils, among which the filter paper (FP) method is relatively uncomplicated and economical. The FP method has also been used in geotechnical engineering applications by several researchers which showed a reliable soil suction measurement. For example, shear modulus behavior of compacted lateritic soil [16], shear strength of an expansive soil by combining the PF method and direct shear tests [17], compacted subgrade soil [18], and compacted loess soil [19].

Thus, the objective of this paper is to investigate on the SWRC and permeability function prediction of four sand-para rubber (SPR) mixtures. A series of laboratory tests including the FP method and falling head test is conducted. Wetting SWRC was tested and best-fitted using the Fredlund and Xing (1994) [20] equation and unsaturated hydraulic conductivity of the SPR mixtures was estimated using the equation of Fredlund et al. (1994) [21]. Finally, the fitting parameters obtained and the PR affected by sand characteristics have been discussed.

(a) (b)

Figure 2: Materials used in this experiment; (a) sand and (b) para rubber.

2. Materials and Methods

2.1 Materials

2.1.1 Sand

The sample of sand used in this study (Fig. 2a) was collected from the Songkhla Province area, Southern Thailand. The grain size distribution curve of sand is displayed in Fig. 3. The particle size ranged from 0.150 to 1.200mm. Sand is classified as poorly graded sand (SP) according to USCS classification. The coefficient of uniformity (C_u), coefficient of curvature (C_c), specific gravity (G_s), effective grain size (D_{10}), and other soil properties are presented in Table 1.

Table 1. Physical and mechanical properties of sand used in this experiment.

Properties	Value
Specific gravity, G_s	2.640
D_{10} (mm)	0.260
D_{50} (mm)	0.430
D_{60} (mm)	0.480
Coefficient of uniformity, C_u	1.846
Coefficient of curvature, C_c	1.068
Minimum void ratio, e_{min}	0.640
Maximum void ratio, e_{max}	0.880
Minimum dry density, ρ_{dmin} (g/cm^3)	1.399
Maximum dry density, ρ_{dmax} (g/cm^3)	1.603
Soil type (USCS)	Poorly graded sand (SP)

2.1.2 Para rubber

Para rubber latex (Fig. 2b) is a stable colloidal dispersion of polymeric materials in an aqueous medium and that is commercially available [22]. High ammonia centrifuged latex was used in this study with ammonia content of 0.700%. The significant physicochemical parameters (Table 2) comprise dry rubber content (DRC) of 60.050%, total solid content (TSC) of 61.730%, volatile fatty acid (VFA) number of 0.024, alkalinity, potassium hydroxide (KOH) number of 0.645, a viscosity of 59.200 centipoises, and specific gravity (at 25°C) of 0.945.

2.2 Experiment program

A report of Lukjan et al. (2019) [12] indicated that a PR content about 18% by weight of dry sand yields

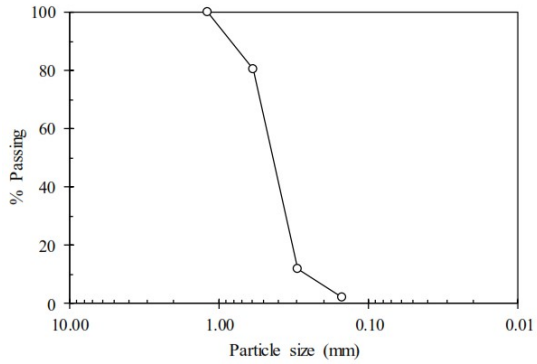

Figure 3: Grain size distribution curve of the poorly graded sand.

an optimum content which improved shear strength of the poorly graded sand. Therefore, sand-para rubber (SPR) mixture of four mix proportions was prepared in this experiment. In preparation for wetting SWRC and permeability tests, sand was oven-dried at 105 °C for 24 h before mixing with PR. Four SPR mixtures include SPR15, SPR17.5, SPR20, and SPR22.5 corresponding to the PR content of 15, 17.5, 20, and 22.5% by weight of dry sand, respectively (Table 3). Soil suction measurement and permeability tests are described as following.

Table 2. Physicochemical parameters of para rubber.

Properties	Value
Dry rubber content, DRC (%)	60.050
Total solid content, TSC (%)	61.730
Ammonia content (%)	0.700
Volatile fatty acid number, VFA	0.024
KOH number	0.645
Viscosity (cps.)	59.200
Specific gravity at 25 °C	0.945

Table 3. Description of sand-para rubber (SPR) mixtures used in this experiment.

Mixtures	PR content (%)	Initial Dry density (g/cm^3)
SPR15	15	1.441
SPR17.5	17.5	1.520
SPR20	20	1.544
SPR22.5	22.5	1.460

2.2.1 Soil suction measurement

The sample high affected in the SWRC test was suggested by Silva et al. (2018) [23] which recommended using soil samples not more than 25 mm. Therefore, the tests were performed with a sample of 60.500mm diameter and 12.500mm height. The preparation process of the SPR specimens comprised: (1) weighing and mixing sand with PR at a specific proportion; (2) tamped with 25 strokes of tamping rod in a mold; (3) oven-dried at 105 °C for 24 h and then allowed to cool at room temperature; (4) wetted by spraying water on the dried SPR specimens to achieve a series of a targeted degree of saturation approximately 10% to 90%; (5) sealed inside plastic jars at 25 °C room for 48 h to ensure the moisture equalization and; (6) conducted following the filter paper method procedure according to ASTM D5298-03 [24]. This study, 55mm diameter of Whatman Grade 42 filter paper is used to measure the matric suction (direct-contact method). Left the SPR samples for 10 days to ensure a thorough equilibrium. Finally, the matric suction value is derived from the ASTM calibrated water retention curve of the filter paper and then the volumetric water content of the soil is calculated by the Eq. (1). Fig. 4 demonstrate the procedures of the FP method.

$$\theta_w = w\,(\rho_d/\rho_w) \tag{1}$$

where θ_w = the volumetric water content of soil; w = gravimetric water content of soil; ρ_d = dry density of soil; and ρ_w = density of water (1 g/cm^3).

2.2.2 Soil permeability test

The specimens used for the permeability test were separated into 2 groups, namely: (i) the pure sand for the constant head test according to ASTM D2434 [25] and (ii) the SPR samples for falling head test according to ASTM D5084 [26]. Only the procedure of the test for SPR samples was described in this paper. The SPR specimen preparation and falling head test consist of 5 main steps: (1) mixed sand with PR by a ratio as well as the FP method; (2) each mixed, contained the sample that divides into two layers in a cylinder mold of 70 mm in diameter and 75 mm in height and tamped with tamping rod of 25 blows/layer; (3) oven-dried at 105 °C for 48 h and then allowed to cool at room temperature; (4) soaked at room temperature in a water bath for 48 h to ensured saturation; (5) tested following ASTM standard method and calculated saturated hydraulic conductivity. Fig. 5 represents the falling head test procedures of the SPR specimens.

2.3 Fitting of the SWRC data

Among all the existing SWRC equations, Fredlund and Xing equation has been suggested by Leong and Rahardjo (1997) [27] which cover a wide range of soils over the entire range of matric suction. Therefore, the Fredlund and Xing's equation in SEEP/W numerical software [28] was adopted in this study to characterize the SWRC of the SPR samples. Eq. (2) present the Fredlund and Xing (1994) [20] equation for SWRC.

$$\theta_w = \theta_s \left[1 - \frac{\ln(1+\psi/\psi_r)}{\ln(1+10^6/\psi_r)}\right]\left[\frac{1}{\{\ln[e+(\psi/a)^n]\}^m}\right] \tag{2}$$

in which θ_w = volumetric water content at any suction; θ_s = saturated volumetric water content; e = the natural number (2.71828...); ψ = any soil suction (kPa); ψ_r = residual soil suction (kPa) corresponding to the

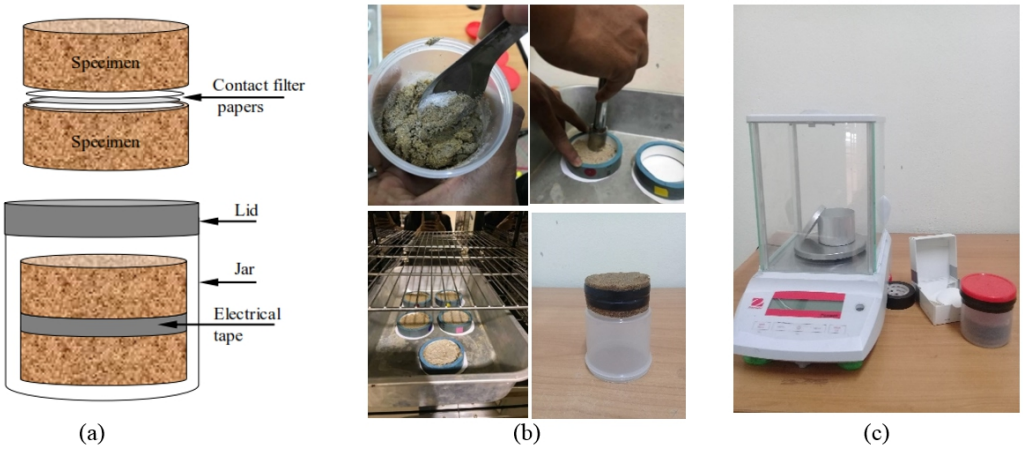

Figure 4: Filter paper method: (a) test configuration; (b) the SPR specimen preparation and; (c) suction measurement set up.

Table 4. Soil water retention curve model fit parameters.

Description	Symbol	SP	SPR15	SPR17.5	SPR20	SPR22.5
Saturated volumetric water content	θ_s	0.282	0.292	0.309	0.332	0.334
Volumetric water content at ψ_w	$\theta_{\psi w}$	0.015	0.070	0.072	0.080	0.085
Wetting saturated point (kPa)	ψ_{bw}	2.100	2.800	1.800	2.200	3.420
Water-entry value (kPa)	ψ_w	6.900	9.050	10.150	11.500	11.800
Fredlund and Xing best fit parameters	a(kPa)	2.977	3.325	2.451	3.077	3.972
	m	1.345	0.534	0.561	0.609	0.486
	n	4.797	5.842	3.884	3.652	6.871

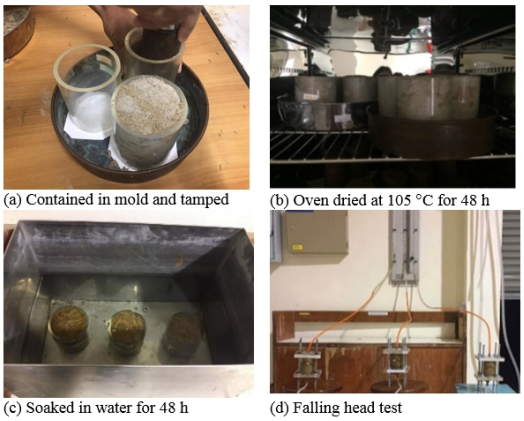

Figure 5: The procedures of the falling head test.

residual water content, θ_r ; and a, m, n = fitting parameters.

2.4 *Prediction methods of unsaturated hydraulic conductivity*

Permeability function of unsaturated soil is known as a relationship of hydraulic conductivity varies with the changes in matric suction. SWRC and permeability function is required for analyses of water flow throughout soil pores concerning variations in matric suctions. In this paper, the indirect measurement based on the statistical predictive methods proposed by Fredlund et al. (1994) in SEEP/W program [28] for unsaturated hydraulic conductivity was used to determine the permeability function from SWRC together with the saturated permeability of the SPR mixtures. The equation proposed by Fredlund et al. (1994) [21], consists of developing the unsaturated hydraulic conductivity function by integrating along the entire curve of the volumetric water content function, is as shown in Eq. (3).

$$k_w = k_{sat}\left[\frac{\int_{\ln(\psi)}^{b}\left[\theta(e^y)-\theta(\psi)\right]/e^y\theta'(e^y)dy}{\int_{\ln(\psi_{aev})}^{b}\left[\theta(e^y)-\theta_s\right]/e^y\theta'(e^y)dy}\right] \quad (3)$$

where k_w = unsaturated hydraulic conductivity for a specified water content or soil suction (m/s); k_{sat} = measured saturated hydraulic conductivity (m/s); ψ = soil suction (function of volumetric water content, θ); θ_s = saturated volumetric water content; e = the natural number (2.71828...); y = dummy variable of integration representing the logarithm of suction, θ' = the first derivative of the Eq. (1), $b = ln(10^6)$; and ψ_{aev} = air entry value.

3. Result and Discussion

3.1 *Wetting SWRC*

When soil is in a wetting stage, as water infiltrates the soil structure and displaces pore air, the water con-

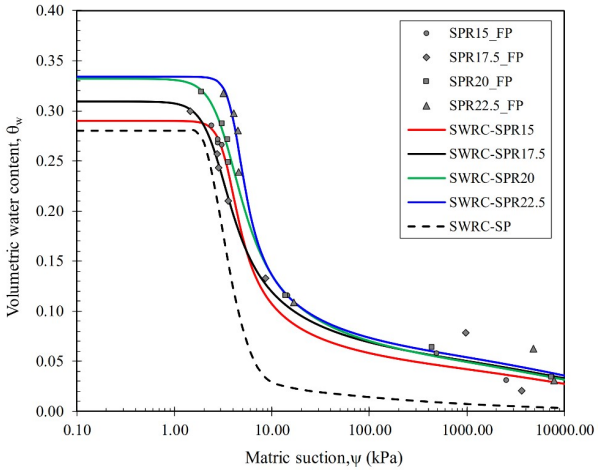

Figure 6: Soil water retention curve of the sand-para rubber (SPR) mixtures.

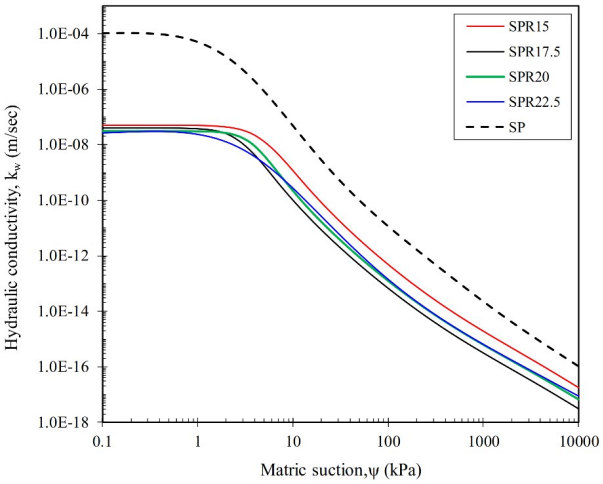

Figure 8: Unsaturated hydraulic conductivity function of sand-para rubber (SPR) mixtures.

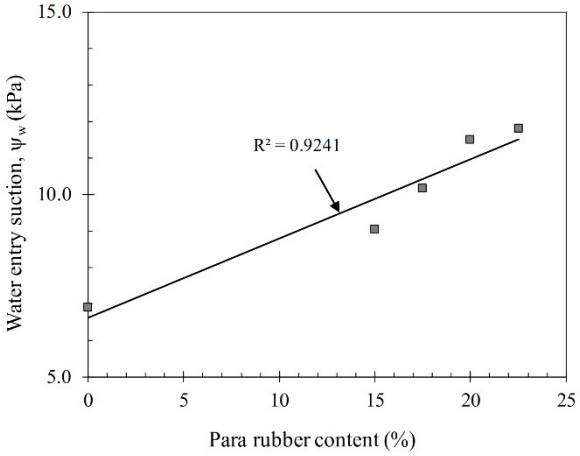

Figure 7: Water entry suction corresponds to the PR content of the wetting SWRCs.

tent will gradually increase [29]. In this study, the wetting SWRCs were obtained for the four SPR mixtures using the FP method. For the poorly graded sand, the SWRC was estimated by using the SEEP/W numerical program based on the grain-size distribution method which used the parameter obtained in Table 1 include grain size of D_{10} and D_{60}. The SWRC parameters fitting are summarized in Table 4. The experimental data and the best-fit SWRC results of the SPR mixtures are depicted in Fig. 6. The results show that the SWRC of the four SPR mixtures has significantly different compared with untreated sand (SP) which tends to give a higher value of saturated volumetric water content (θ_s) at low matric suction. Such increasing included about 3%, 10%, 18%, and 19% for the SPR mixtures of SPR15, SPR17.5, SPR20, and SPR22.5, respectively. The water entry value (ψ_w) is the suction at which the water content of soil starts to increase in the adsorption process. From the result in Fig. 7 indicates the value of ψ_w increases of 31%, 47%, 67%, and 71% for the SPR mixtures of SPR15, SPR17.5, SPR20, and SPR22.5, respectively. This implies that the PR causes the sand to reduced pore size. Increasing the values of volumetric water content (both θ_s and $\theta_{\psi w}$) of the SPR specimens demonstrated the effect of the water-holding capacity to the sand of para rubber. In other words, the high amount of water retained due to the water-absorption of the PR.

The absorption behavior for all mixtures found that there is some variability of the SWRC for each zone, especially in the transition zone. Water content increases moderately in the residual zone ($\psi > 12$ kPa) although soil suction decreases by several orders of magnitude. This is because pores have high capillary tension as a result of small sizes. In the transition zone ($\psi \approx 2 - 12$ kPa), water content increased rapidly rate with suction decrease. Compared the SWRCs among all mixtures found that there are variations of water content and suction in this zone. Such as the smallest of ψ_{bw} value of the SPR17.5. For the capillary saturation zone ($\psi < 2$ kPa), the soil suction almost be unchanged which found that having increased saturated water content mention above.

3.2 Measured saturated hydraulic conductivity

The permeability testing includes constant head and falling head test methods. The testing results of the sand sample (SP) and the SPR mixtures are shown in Table 5. The initial saturated hydraulic conductivity (k_{sat}) of SP is 6.890×10^{-5} m/s. The values of k_{sat} generally decreased with increasing PR content. Addition of 15%, 17.5%, 20%, and 22.5% PR contents to SP sand decreases its k_{sat} about 3 orders of magnitude. Overall, the ranges in the measured ksat for the SPR mixtures varied from 4.890×10^{-8} m/s (SPR15) to 2.280×10^{-8} m/s (SPR22.5). The results implied that PR has the potential for permeability control of sand.

Table 5. Summary of the hydraulic conductivity values obtained from laboratory testing and permeability function prediction.

Description	Symbol	SP	SPR15	SPR17.5	SPR20	SPR22.5
Saturated hydraulic conductivity (m/sec)	k_{sat}	6.890e-05	4.890e-08	3.960e-08	3.100e-08	2.280e-08
Unsaturated hydraulic conductivity at wetting saturated point (m/sec)	$k_{\psi bw}$	1.500e-05	3.520e-08	3.020e-08	2.000e-08	1.250e-08
Unsaturated hydraulic conductivity at water-entry value point (m/sec)	$k_{\psi w}$	2.800e-07	2.000e-10	1.000e-10	1.420e-10	1.800e-10

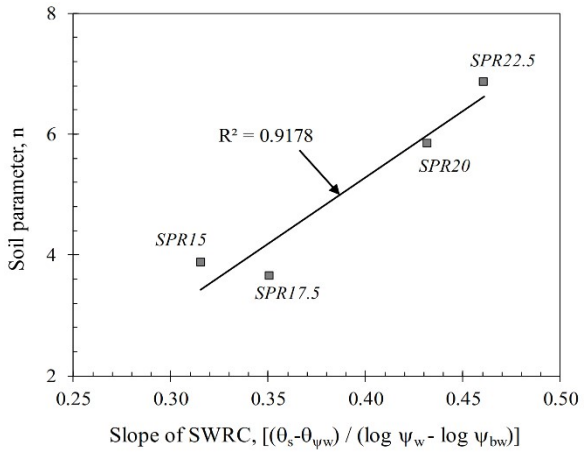

Figure 9: Slope of sand-para rubber (SPR) mixtures.

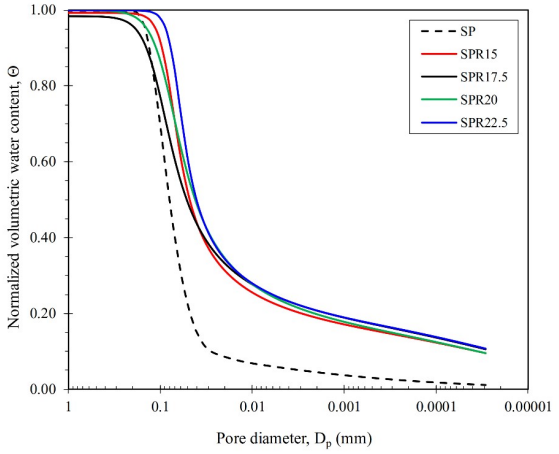

Figure 10: Pore size via normalized volumetric water content of sand-para rubber (SPR) mixtures.

3.3 Prediction and analysis of permeability function

Using the SWRC fitting parameters summarized in Table 4 and the saturated hydraulic conductivity obtained from the laboratory test described in the previous section, the unsaturated hydraulic conductivity (k_w) was predicted using the equation of Fredlund et al. (1994) [21]. Fig. 8 displays the k_w values of four SPR mixtures and the SP sand concerning matric suction. The shape of the curve is quite similar for all SPR mixtures but values vary in three orders of magnitudes compared with a value of untreated sand. The value of unsaturated hydraulic conductivity at wetting saturated point $k_{\psi bw}$ (Table 5) is decreased with the PR content increased.

3.4 Effect of PR on the pore size distribution

To describe the influence of PR content on the shape of SWRC, the slope and pore size variations were discussed. Generally, the slope of the SWRC describes the rate of water lost from the soil (drying) or filled in pores (wetting) [30]. The steeper slope of the SWRCs, larger the parameter n. The slope of wetting SWRC can be calculated as $\left[(\theta_s - \theta_{\psi w})/(\log \psi_w - \log \psi_{bw})\right]$, as depicted in Fig. 9. Yang et al. (2004) [31] reported that the SWRC of a uniform soil has a steeper slope than that of a less uniform soil. In this study, the shape of the SWRCs (Fig. 9) of the pure sand has a slightly steeper slope than that of the SPR mixtures. For SP sand, the slope of SWRC has a consistent to grain-size distribution whereas that slope reduces with the SPR mixtures. Since the shape of SWRC is related to pore size [30]. The pore size diameter can be calculated from the Laplace's equation of $\left[D_p = 4T_s \cos\alpha/\psi\right]$, in which T_s = surface tension of water (72.750 mN/m at 20 °C), α is the contact angle between pore water and particles which can be 0 for water-soil interface. Fig. 10 presents the relationship between pore size distribution and the normalized volumetric water content [$\Theta = \theta_w/\theta_s$]. The pore size ranged from 3.000e-05 to 1 mm. For the same water content, the D_p of the SPR mixtures is evidence smaller than that of SP sand which exhibits the presence of the PR.

4. Conclusions

The wetting soil water retention curves (SWRCs) using the filter paper method and the falling head test of the SPR mixtures were conducted in this study. The experimental results showed that the PR contents have prominent effects on the SWRC of poorly graded sand. Increasing the volumetric water content of the SPR mixtures represented the effect of the water-holding capacity to the sand of para rubber. The saturated hydraulic conductivity reduced about 3 orders of magnitude when sand was treated with the PR. The unsaturated hydraulic conductivity prediction based on the statistical method showed the evident effected of the para rubber biopolymer. The decrease of the hydraulic conductivity and pore size of the SP sand suggest the significant potential of the PR that can be applied for various geotechnical engineering applica-

tions such as sandy soil stabilization, surface erosion reduction, sand liquefaction, and so on.

Acknowledgment

The authors gratefully acknowledge the Faculty of Engineering, the Rajamangala University of Technology Srivijaya for providing laboratory facilities in this study.

References

[1] G. A. Siemens, Thirty-Ninth Canadian Geotechnical Colloquium: Unsaturated soil mechanics-bridging the gap between research and practice, Canadian Geotechnical Journal 55 (2018) 909 - 927.

[2] A. F. Cabalar, M. Wiszniewski, Z. Skutnik, Effects of xanthan gum biopolymer on the permeability, odometer, unconfined compressive and triaxial shear behavior of a sand, Soil Mechanics and Foundation Engineering 54(5) (2017) 356 - 361.

[3] J. Jang, A review of the application of biopolymers on geotechnical engineering and the strengthening mechanisms between typical biopolymers and soils, Advances in Materials Science and Engineering (2020).

[4] I. Chang, A. K. Prasidhi, J. Im, G. C. Cho, Soil strengthening using thermo-gelation biopolymers, Construction and Building Materials 77 (2015) 430 - 438.

[5] I. Chang, G. C. Cho, Shear strength behavior and parameters of microbial gellan gum-treated soils: from sand to clay, Acta Geotechnica 14(2) (2019) 361 - 375.

[6] S. Lee, J. Im, G. C. Cho, I. Chang, laboratorytriaxialtest behavior of xanthan gum biopolymer-treated sands, Geomechanics and Engineering 17(5) (2019) 445 - 452.

[7] M. B. Burbank, T. J. Weaver, T. L. Green, B. C. Williams, R. L. Crawford, Precipitation of calcite by indigenous microorganisms to strengthen liquefiable soils, Geomicrobiology Journal 28 (2011) 301 - 312.

[8] E. KavazanjianJr, E. Iglesias, I. Karatas, Biopolymersoil stabilization for wind erosion control, Proceedings of the 17th International Conference on Soil Mechanics and Geotechnical Engineering, 2009, pp. 881 - 884.

[9] S. M. Ham, I. Chang, D. H. Noh, T. H. Kwon, B. Muhunthan, Improvement of surface erosion resistance of sand by microbial biopolymer formation, Journal of Geotechnical and Geoenvironmental Engineering 144(7) (2018).

[10] R. Khachatoorian, I. G. Petrisor, C. C. Kwan, T. F. Yen, Biopolymer plugging effect: laboratory-pressurizedpumping flow studies, Journal of Petroleum Science and Engineering 38(1-2) (2003) 13 - 21.

[11] A. Bouazza, W. P. Gates, P. G. Ranjith, Hydraulic conductivity of biopolymer-treated silty sand, Geotechnique 59 (1) (2009) 71 - 72.

[12] A. Lukjan, A. Iyaruk, S. Swasdi, C. Somboon, Shear strength characteristics of the natural rubber bonded sand, Engineering Journal of Research and Development 29(4) (2018) 5 - 18. (in Thai)

[13] P. Promputthangkoon, A. Rungvichaniwat, N. Kaewthai Andrei, T. Kuasakul, On the mechanical properties of para rubber-oil palm ash derived geosynthetic clay liner, IOP Conf. Series: Materials Science and Engineering 773 (2020) 012054.

[14] Department of Highway, Specification for natural rubber modified soil cement base course, (2017). (in Thai)

[15] P. Plangoen, Application of rubber latex and soil cement develop drought relieving water pond, Engineering Journal Chiang Mai University 25(2) (2018) 170 - 180. (in Thai)

[16] S. R. Yang, H. D. Lin, J. H. S. Kung, J. Y. Liao, Shear wave velocity and suction of unsaturated soil using bender element and filter paper method, Journal of GeoEngineering 3(2) (2008) 67 - 74.

[17] Q. F. Bai, S. H. Liu, Measurement of the shear strength of an expansive soil by combining a filter paper method and direct shear tests, Geotechnical Testing Journal 35(3) (2012) 451 - 459.

[18] H. Kim, E. Ganju, D. Tang, M. Prezzi, R. Salgado, Matric suction measurements of compacted subgrade soils, Road Materials and Pavement Design 16(2) (2015) 358 - 378.

[19] X. Xie, P. Li, X. Hou, T. Li, G. Zhang, Microstructure of compacted loess and its influence on the soil-water characteristic curve, Advances in Materials Science and Engineering (2020).

[20] D. G. Fredlund, A. Xing, Equations for the soil-water characteristic curve, Canadian Geotechnical Journal 31 (1994) 521 - 532.

[21] D. G. Fredlund, A. Xing, S. Huang, Predicting the permeability function for unsaturated soils using the soil-water characteristic curve, Canadian Geotechnical Journal 31 (1994) 533 - 546.

[22] P. Sirisomboon, C. H. Lim, Rapid evaluation of the properties of natural rubber latex and its products using near-infrared spectroscopy, (2019) In Organic Polymers. IntechOpen.

[23] M. L. D. N. Silva, P. L. Libardi, F. H. S. Gimenes, Soil water retention curve as affected by sample height, Revista Brasileira de Ciencia do Solo 42 (2018).

[24] ASTM D5298-03, Standard test method for measurement of soil potential (suction) using filter paper, ASTM International, West Conshohocken, PA, 2003.

[25] ASTM D2434-19, Standard test method for permeability of granular soils (constant head), ASTM International, West Conshohocken, PA, 2019.

[26] ASTM D5084-16a, Standard test methods for measurement of hydraulic conductivity of saturated porous materials using a flexible wall permeameter, ASTM International, West Conshohocken, PA, 2016.

[27] E. C. Leong, H. Rahardjo, Review of soil-water characteristic curve equations, Journal of Geotechnical and Geoenvironmental Engineering 123(12) (1997) 1106 - 1117.

[28] GEOSTUDIO, User's Manual, Geo-slope international Ltd. Calgary, Alberta, 2012.

[29] W. L. Xiea, P. Lia, S. K. Vanapallib, J. D. Wanga, Prediction of the wetting-induced collapse behaviour using the soil-water characteristic curve, Journal of Asian Earth Sciences 151 (2018) 259 - 268.

[30] S. S. Agus, E. C. Leong, H. Rahardjo, Soil-water characteristic curves of Singapore residual soils, Geotechnical and Geological Engineering 19 (2001) 285 - 309.

[31] H. Yang, H. Rahardjo, E. C. Leong, D.G. Fredlund, Factors affecting drying and wetting soil-water characteristic curves of sandy soils, Canadian Geotechnical Journal 41 (2004) 908 - 920.